Scientific Report No. 44

TRANSIENT ELECTROMAGNETIC FIELD GENERATED BY A VERTICAL ELECTRIC DIPOLE ON THE SURFACE OF A DISSIPATIVE EARTH

by

Hussain Haddad and David C. Chang

February 1979

Electromagnetics Laboratory
Department of Electrical Engineering
University of Colorado
Boulder, Colorado 80309

Abstract

Transient response of a vertical dipole source with an impulse excitation is obtained. Both the dipole and other observation points are assumed to be located on the surface of a homogeneous dissipative earth. It is shown that the response consists of two distinct waves; one arriving from a path in air and the other in earth. The latter is found usually to be several orders smaller in a typical situation. On the other hand, with the use of an alternative integral representation, numerical integration of double infinite integrals associated with the Sommerfeld problem can be reduced to single integrals of finite extent. The role of the Zenneck wave in the time domain is also explained.

TABLE OF CONTENTS

TRANSIENT ELECTROMAGNETIC FIELD GENERATED BY A VERTICAL ELECTRIC DIPOLE ON THE SURFACE OF A DISSIPATIVE EARTH

Hussain Haddad and David C. Chang

1. Introduction

Recently, considerable interest has been given to the study of electromagnetic transients. Some of these studies are motivated by the desire to provide adequate protection of electronic equipment in a strong electromagnetic pulse (EMP) [1]. Other studies have been applied to the probing of fields in geological media [2], determination of the current in a lightning return stroke [3], the detection of nuclear bursts [4] and the discrimination of a radar scatterer [5].

In this paper we are interested in the problem of an electromagnetic pulse propagation on a lossy half-space generated by a vertical dipole. A classical work in this area is that of Van der Pol [6], for the transient field over a non-conducting earth generated by a vertical dipole source situated in the interface between the air and the earth. In later papers [7]-[8], the transient solution of an elevated dipole was also obtained. Wait [9,10] and Novikov [11] studied the transient response of a vertical dipole with a step or ramp function current source over a finitely conducting earth. Since the Sommerfeld-Norton ground wave expansion is employed, which is valid for distances large compared with the free space wavelength, his result is expected to be accurate mainly in the very early time portion of the response. Approximate expression for the transient field at later observation times was found by Chang [12] and Wait [13], under the assumption that the

dissipative half-space can be replaced by an impedance surface. Fuller and Wait [14], subsequently extended the problem into an actual earth environment where the conductivity and permittivity of earty vary as a function of frequency, based upon asymptotic expansions of the field in the frequency domain.

From the above discussion, it becomes apparent that only approximate expressions of the transient field response have been obtained; each is valid in a selected range of parameters and none is valid for a more general case. Basically, the main difficulty which prevents an "exact" evaluation, arises because the frequency-domain solution of such a problem involves infinite integrals that can not be expressed in closed-form. Thus, the time-domain solution can be obtained only in principle by carrying out another infinite integration in the frequency domain. Hence a direct numerical evaluation of these double-infinite integrals becomes rather impractical.

In this work, we shall develop an efficient numerical scheme for the computation of these integrals. This involves initially the study of the spectral properties of the Sommerfeld integral in the complex frequency domain. Deformation of the integration contour in the lower half of the complex plane not only reduces the double infinite integrals to finite integrals, but also enables us to carry out one of the integrations analytically in closed form. Consequently, we are able to compute the electric and magnetic responses for cases typically encountered in a general earth environment. Our approach conceptually can be considered as an extension of the Singularity Expansion Method (SEM) [30] technique to problems involving, non-isolated singularities (branch cuts) in the complex frequency domain.

2. Formulation

We first consider the time-harmonic field due to a vertical electric Hertzian dipole of dipole moment $\tilde{I}(\omega)d\ell$, located on the surface of a dissipative half-space (earth) having a conductivity σ and permittivity $\varepsilon = \varepsilon_o\varepsilon_r$. The upper half-space is assumed to be air (Fig. 1). A cylindrical coordinate (r,ϕ,z) is employed and a time-factor of $\exp(-i\omega t)$ is used. Expression for the time-harmonic Hertzian potential of electric type, observed also on the earth surface, can be found in [15], or originally by Sommerfeld [16] as consisting of only a z-component:

$$\tilde{\pi}_z(r;\omega) = \frac{i\omega\mu_o k_1^2 \tilde{I}(\omega)d\ell}{4\pi k_o^2} V(r;\omega), \tag{1}$$

where

$$\tilde{V}(r;\omega) = 2\int_o^\infty [k_o^2\gamma_1 + k_1^2\gamma_o]^{-1} J_o(\alpha r)\, \alpha d\alpha.$$

$$\gamma_{o,1} = (\alpha^2 - k_{0,1}^2)^{\frac{1}{2}} \quad \text{with } \mathrm{Re}(\gamma_{o,1}) \geq 0 ,$$

and

$$k_o = \frac{\omega}{C_o} \; ; \quad k_1 = \frac{\omega}{C_1}\left(\frac{\omega+i2\Delta}{\omega}\right)^{\frac{1}{2}}$$

$C_{o,1} = (\mu\varepsilon_{o,1})^{-\frac{1}{2}}$ is the speed of light in air and in earth, respectively; $\Delta = \sigma/2\varepsilon_r\varepsilon_o$ is associated with the inverse of the relaxation time in a dissipative medium, and J_o is the Bessel function of order zero. We note that depending upon the particular absorption model chosen Δ is not necessarily independent of the operating frequency ω. However, we do have to require the square root in k_1 be so chosen so that it approaches $+1$ as $|\omega| \to \infty$. In (1), we have also dropped the dependence on z and ϕ, since we are only interested in those observations made on the earth surface.

The time-dependent z-component of the electric field and the ϕ-component of the magnetic field in the interface can be found once the real-time solution of the vector potential given above is obtained. These field

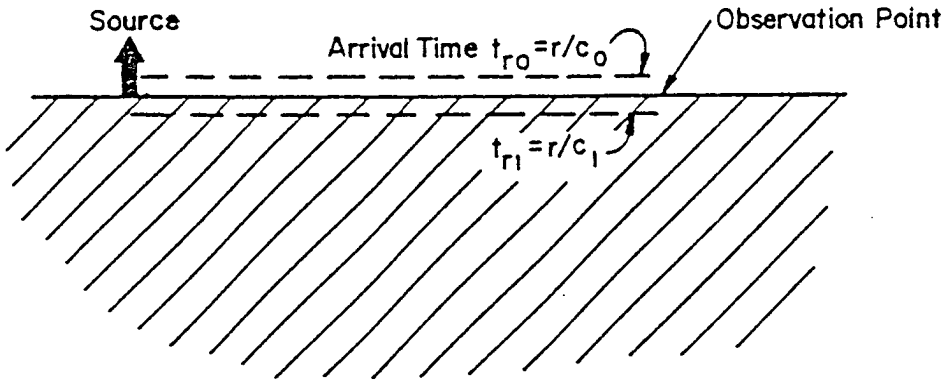

Figure 1. Source and observation point located on the ground surface.

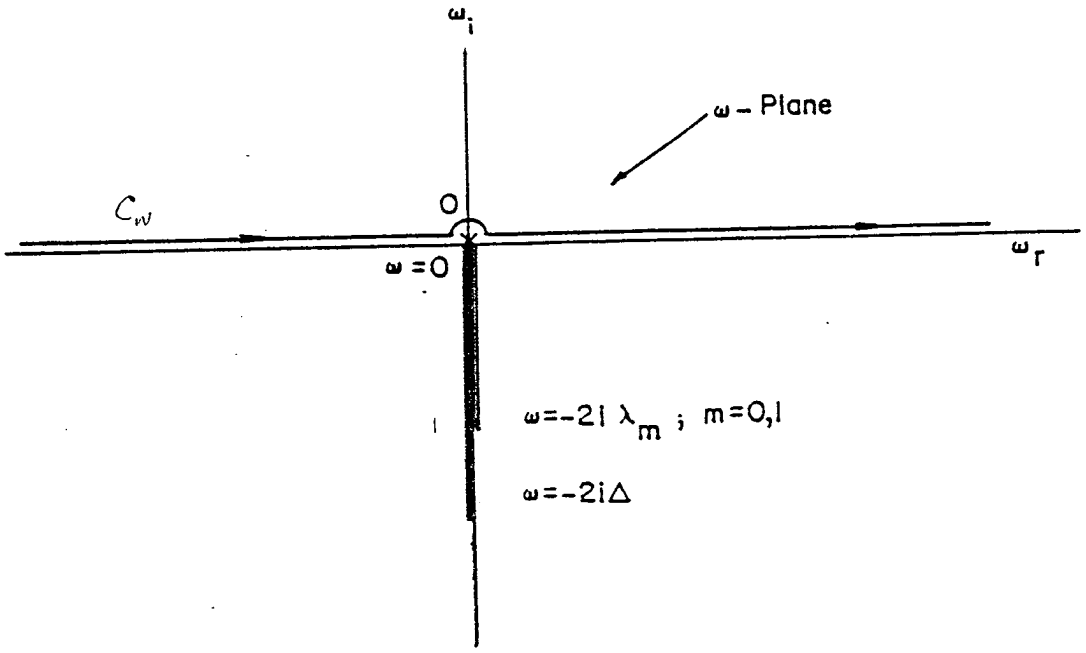

Figure 2. Singularities in the complex ω-plane

components can be described in cylindrical coordinate systems as follows.

$$E_z = -\frac{1}{r}\frac{\partial}{\partial r}\, r\,\frac{\partial}{\partial r}\,\pi_z(r;t) \tag{2}$$

$$H_\phi = -\varepsilon_o\,\frac{\partial^2}{\partial t\,\partial r}\,\pi_z(r;t) \tag{3}$$

where $\pi_z(r;t)$ is obtained from the use of the Fourier-Laplace transform

$$\pi_z(r;t) = \int_{C_w} \pi_z(r;\omega)e^{-i\omega t}d\omega \tag{4}$$

Here C_w is specified along the real axis of the complex ω-plane as shown in Fig. 2. As evident from the substitution of (1) into (4), the real time expression $\pi_z(r,t)$ involves the double infinite integration over both α and ω, which obviously cannot be evaluated efficiently in a computer without further modification.

Because of the identity [17], $2J_o(z) = H_o^{(1)}(z) + H_o^{(1)}(ze^{i\pi})$, where $H_o^{(1)}$ is the Hankel function of the first kind and order zero, we can replace the integral in (2) by

$$\tilde{V}(r,\omega) = \int_{\infty}^{\infty} [k_o^2\gamma_1 + k_1^2\gamma_o]^{-1}\, H_o^{(1)}(\alpha r)\alpha d\alpha \tag{5}$$

provided that a branch-cut is defined along the negative real axis and the integration path is specified as slightly above the negative real axis in the α-plane. The new representation will then allow us to deform the path of integration into the upper half of the complex α-plane, which obviously can be separated into contributions from branch-cuts associated with the square root functions γ_o and γ_1 plus the residue contribution from pole singularity at α_p; where $\alpha_p = k_1\, k_1/(k_1^2 + k_o^2)^{\frac{1}{2}}$ (see Fig. 3). For a time-harmonic field of operating frequency ω, the residue contribution from α_p is commonly known as the "Zenneck wave," which constitutes a legitimate solution of Maxwell equation that satisfies the boundary

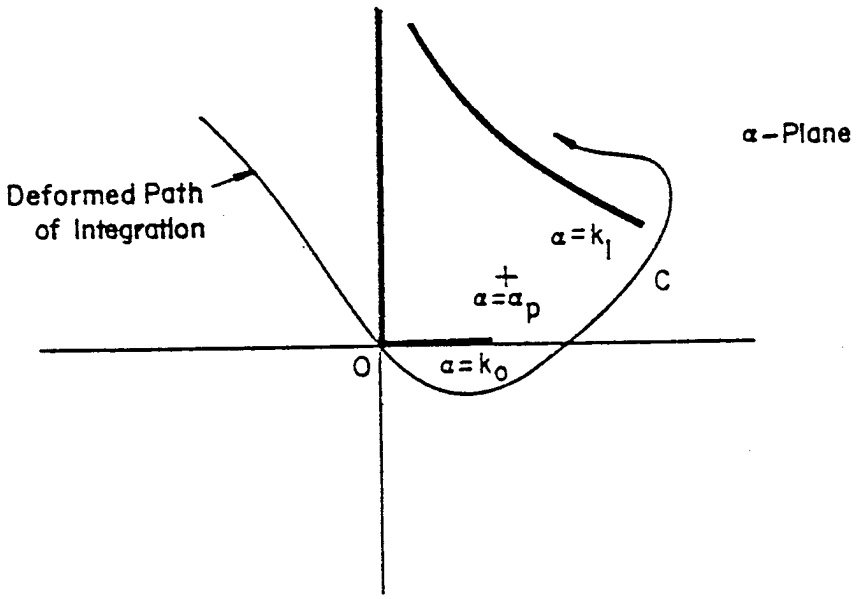

Figure 3. Deformation of the real axis path of integration into the contour C in the upper half of the complex α-plane.

conditions at the interface and is confined to the finite spatial domain (i.e. decays exponentially away from the interface). Furthermore, it can be excited realistically by a dipole source, along with the radiation fields into air and earth regions associated with the two branch-cut integrations. If taken individually in the calculation of the transient response, one immediately concludes that such a term will have an arrival time of r/c_p, where $c_p = \lim_{|\omega|\to\infty} (\omega/\alpha_p) = (c_o^2 + c_1^2)^{\frac{1}{2}}$, which clearly violates the physical principle of time causality, and hence can not exist independently. We have to realize however, arrival times are closely associated with the behaviour of the field at $|\omega| \to \infty$. From Fig. 3, it is not difficult to see that the branch point $\alpha = k_1 = [\omega(\omega + i2\Delta)]^{\frac{1}{2}}/c_1$, also approaches the real axis in the α-plane in the limit of $|\omega| \to \infty$ so that the Zenneck-wave pole is now more and more "sandwiched" between the two cuts. By cancelling the contribution from the pole with the integration along the adjacent sides of the two branch cuts in the vicinity of the pole, the effect of the pole actually becomes indistinguishable from those of the cuts.

Thus, instead of getting separately the contribution of the branch cuts and the residue contribution of the pole, we will evaluate the integral somewhat differently. Noticing that the denominator of (7) can be rearranged to give

$$\frac{1}{k_o^2 \gamma_1 + k_1^2 \gamma_o} = \frac{1}{k_1^4 - k_o^4}\left[\frac{k_1^2}{\gamma_o} + \frac{k_1^2(\alpha_p^2 - k_o^2)}{\gamma_o(\alpha^2 - \alpha_p^2)} - \frac{k_o^2}{\gamma_1} - \frac{k_o^2(\alpha_p^2 - k_1^2)}{\gamma_1(\alpha^2 - \alpha_p^2)}\right] \qquad (6)$$

We can consider $\tilde{\pi}_z(r;\omega)$ as constituted of four fundamental integrals, i.e.

$$\tilde{\pi}_z = \frac{\eta_o F(\omega) d\ell}{2\pi} \sum_j \tilde{S}_j(r;\omega) \ , \qquad (7)$$

$$\tilde{S}_1 = -\frac{c_o N(\omega)}{2\omega^2}\int_{\infty}^{\infty}\frac{1}{\gamma_o}\,H_o^{(1)}(\alpha r)\alpha d\alpha \tag{8}$$

$$\tilde{S}_2 = -\frac{c_o N(\omega)}{2\omega^2}(\alpha_p^2 - k_o^2)\int_{\infty}^{\infty}\frac{1}{\gamma_o(\alpha^2-\alpha_p^2)}\,H_o^{(1)}(\alpha r)\alpha d\alpha \tag{9}$$

$$\tilde{S}_3 = \frac{c_o N(\omega)}{2\omega^2}\left(\frac{k_o}{k_1}\right)^2\int_{\infty}^{\infty}\frac{1}{\gamma_1}\,H_o^{(1)}(\alpha r)\alpha d\alpha \tag{10}$$

$$\tilde{S}_4 = \frac{c_o N(\omega)}{2\omega^2}\left(\frac{k_o}{k_1}\right)^2(\alpha_p^2 - k_1^2)\int_{\infty}^{\infty}\frac{1}{\gamma_1(\alpha^2-\alpha_p^2)}\,H_o^{(1)}(\alpha r)\alpha d\alpha \tag{11}$$

where

$$F(\omega) = -i\omega\tilde{I}(\omega); \qquad N(\omega) = \frac{k_1^4}{k_1^4 - k_o^4} \tag{12}$$

and $\eta_o = 120\pi$ ohms is the free-space characteristic impedance. Among the S-integrals, S_1 and S_3 are known analytically in closed form,

$$\tilde{S}_1 = -N(\omega)\,\frac{c_o\, e^{i\omega r/c_o}}{\omega^2 r}; \qquad \tilde{S}_3 = \frac{N(\omega)c_1 e^{i\frac{r}{c_1}[\omega(\omega+i\Delta)]^{\frac{1}{2}}}}{r\omega(\omega+i\Delta)} \tag{13}$$

while $\tilde{S}_2$ and $\tilde{S}_4$ need to be evaluated numerically. As seen from (9), the integral associated with $\tilde{S}_2$ is a special case of $b = 0$ and

$$f(r,b) = \int_{\infty}^{\infty}\frac{e^{-\gamma_o b}}{\alpha^2-\alpha_p^2}\,H_o^{(1)}(\alpha r)\,\frac{\alpha d\alpha}{\gamma_o}; \quad b \geqslant 0 \tag{14}$$

which can be shown without difficulty to satisfy the following differential equation

$$\frac{\partial^2}{\partial b^2} + (k_o^2 - \alpha_p^2)f(r,b) = 2\,\frac{e^{ik_o(r^2+b^2)^{\frac{1}{2}}}}{(r^2+b^2)^{\frac{1}{2}}} \tag{15}$$

and the boundary condition that $\lim_{b\to\infty} f(r,b) = 0$ and $f(r,-b) = f(r,b)$. Thus, we can obtain an alternative form of $f(r,0)$, by solving this inhomogeneous differential equation directly,

$$f(r,o) = -2i\,\frac{k_o^2}{k_o^2 - \alpha_p^2}\int_{o}^{\infty}\frac{e^{ik_e R_o}}{k_e R_o}\,e^{i\omega v/c_o}\,dv \tag{16}$$

where

$$k_e = \frac{\omega}{c_o}\left[\frac{(\omega+i2\lambda_o)}{\omega}\right]^{\frac{1}{2}} \quad ; \tag{17}$$

$$\lambda_o = \frac{n^2\Delta v^2}{(n^2+1)v^2+r^2} \tag{18}$$

and

$$R_o = [(n^2+1)v^2+r^2]^{\frac{1}{2}} \tag{19}$$

where $n = \sqrt{\varepsilon_r}$ is the refractive index of earth. As in the case of k_1, the square root in k_e is chosen so that $\lim_{|\omega|\to\infty} k_e = +\omega/c_o$.

Clearly, the factor $e^{ik_eR_o}/k_eR_o$ represents the potential function of a dipole in a medium with a complex propagation constant k_e. The form of (16) is then equivalent to that of a vertical current source propagating at the speed of light c_o in a medium characterized by k_e (see Fig. 4).

It should be noted that in the expression (16), because $k_e \to \omega/c_o$ as $\omega \to \infty$, the earliest pulse signal comes from the elemental dipole near the bottom of the source, i.e. for $v \simeq 0$. This implies that the first signal arrives at time $t \geq R_o/c_o$. As the pulse travels along the vertical line source the arrival of the response will be delayed by the factor v/c_o from the time $t = R_o/c_o$.

Substitution of (16) into (9) now yields the expression for $\tilde{S}_2$ as:

$$\tilde{S}_2(r,\omega) = -iN(\omega)\int_0^\infty \frac{e^{\,i\,R_o/c_o\,[\omega(\omega+i2\lambda_o)]^{\frac{1}{2}}}}{[\omega(\omega+i2\lambda_o)]^{\frac{1}{2}}}\, e^{i\omega v/c_o}\,\frac{dv}{R_o} \tag{20}$$

At this point, one might ask the question of what is to be gained to go through a tedious process to transform one infinite integral into another one. It is clear, the new infinite integral can be interchanged with the integral over the ω-domain when we apply the inverse Fourier transform

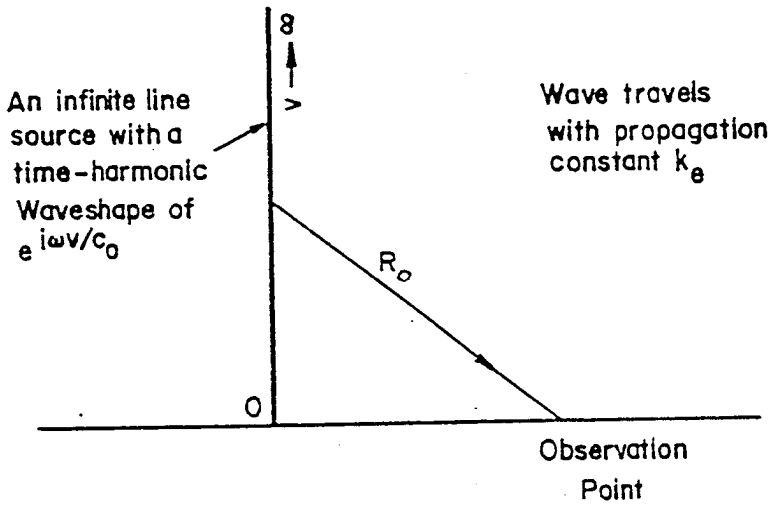

Figure 4. Physical interpretation of the function $f(r,o)$.

to $\pi_z(r;\omega)$ to obtain the time transient solution. As will be seen in the next section such an interchange of the order of integration will allow us to reduce double-infinite integrals into finite, single integrals which certainly would be more suited for numerical computation.

To obtain a proper expression for S_4, we only need to replace the air parameters in (20) by the earth parameters. Following essentially the same steps, we have

$$\tilde{S}_4(r;\omega) = iN(\omega)\int_0^\infty \frac{e^{\,i R_1/c_1 [\omega(\omega + i2\lambda_1)]^{\frac{1}{2}}}}{[\omega(\omega+i2\lambda_1)]^{\frac{1}{2}}} e^{\,i v/c_1 [\omega(\omega+i2\Delta)]^{\frac{1}{2}}} \frac{dv}{R_1} \quad (21)$$

where λ_1 and R_1 are now defined as

$$R_1 = [(1+\frac{1}{n^2})v^2 + r^2]^{\frac{1}{2}} \; ; \quad \lambda_1 = \frac{\Delta(v^2+r^2)}{(1+\frac{1}{n^2})v^2 + r^2} \quad (22)$$

Again the square-root in (21) is so chosen that $[\omega(\omega+i2\lambda_1)]^{\frac{1}{2}} \to \omega$ as $|\omega| \to \infty$.

3. Evaluation in the complex ω-plane:

Following from (7) and (4), the real-time solution of the vector potential can be written as

$$\pi_z(r;t) = 60\, d\ell \sum_{j=1}^{4} \int_{-\infty}^{\infty} \frac{\partial I(t')}{\partial t'} S_j(r;t-t')dt' \quad (23)$$

where

$$S_j(r;t) = \frac{1}{2\pi}\int_\omega \tilde{S}_j(r;\omega)e^{-i\omega t}\, d\omega \quad (24)$$

Thus for a unit step function $I(t) = I_o u(t)$ (where $u(t) = 0$ for $t < 0$ and $u(t) = 1$ for $t \geq 0$) or an impulse function $I(t) = I_o\delta(t)$, the time transients response can be described simply as

$$\pi_z(r;t) = 60\, I_o d\ell \sum_{j=1} S_j(r;t); \quad \text{for a unit step current} \tag{25}$$

and

$$\pi_z(r;t) = 60\, I_o d\ell \sum_{j=1}^{4} \frac{\partial}{\partial t} S_j(r;t); \quad \text{for an impulse current} \tag{26}$$

Once $S_j(r;t)$ as defined in (24) is evaluated, the real time response of the vector potential π_z can be found from the above expressions or thereafter find the electric and magnetic field through the use of (2) and (3) respectively.

We now proceed to evaluate $S_j(r;t)$ through the deformation of the real axis ω-integral into the upper and lower half of the complex ω-plane. To simplify the computation procedure, we shall assume in what follows that both ε_r and σ is independent of ω, although other absorption models can be treated in a similar manner. As seen from (13), (20) and (21), the time-harmonic function $S_j(r;\omega)$, $j = 1,2,3$ or 4 possesses poles, branch cuts or both types of singularities. One type of singularity comes from the function $N(\omega)$ as defined in (12). For a more realistic earth model the refractive index of earth, $n = (\varepsilon_r)^{\frac{1}{2}}$ for any given frequency is large compared to 1, typically $n^2 \geq 10$. This means $N(\omega)$ as defined in the expression (13) can be approximated by 1, which then simplifies the evaluation of $S_j(r;t)$. It should be noted that if a more exact solution is needed, the pole contribution of $N(\omega)$ can be easily added. The first function $S_1(r;t)$ as seen from (13) and (24) therefore can be found easily from the residue contribution at $\omega = 0$

$$S_1(r;t) = \frac{c_o}{r}\,(t - \frac{r}{c_o})\; u(t - \frac{r}{c_o}) \tag{27}$$

where $u(t)$ is Heaviside unit step function.

Evaluation of S_3 is somewhat more complicated because of the branch-cut singularity associated with the square root $[(\omega+i\Delta)/\omega]^{\frac{1}{2}}$, which according

to our earlier discussion, should be chosen in such a way so that it approaches +1 as $|\omega| \to \infty$ (see Fig. 2). For $t > r/c_1$, deformation unto the two sides of the branch-cut in the lower ω-plane yields the following expression after some manipulation

$$S_3(r;t) = -\frac{c_1}{r}\left\{\frac{1-e^{-2\Delta t}}{2\Delta} + \frac{1}{\pi}\int_0^{2\Delta} \sin\left(\frac{r}{c_1}[v(2v-\Delta)]^{\frac{1}{2}}\right) e^{-vt}\,\frac{dv}{v(2\Delta-v)}\right\}$$

where the first term in the curly bracket comes from the residue contribution at $\omega = 0$ and $-2i\Delta$, while the second term comes from the branch-cut integration, and the change of variable $\omega = -iv$. For $t < r/c_1$, deformation onto the upper half-plane encloses no singularity so that $S_3(r;t) = 0$. Using the integral representation of $I_o(x)$ where I_o is the modified Bessel function of the first-kind and order zero [17], we can further reduce the expression of S_3 to

$$S_3(r;t) = -\frac{c_o}{n^2 r}\left\{\frac{1-e^{-2\Delta t}}{2\Delta} - \frac{r}{c_1}e^{-\Delta t}\int_0^1 I_o\left(\Delta\left[t^2-\left(\frac{ry}{c_1}\right)^2\right]^{\frac{1}{2}}\right)dy\right\} u\left(t-\frac{r}{c_1}\right) \tag{28}$$

where $n^2 = \varepsilon_r$, $\Delta = \sigma/2\varepsilon_r\varepsilon_o$ and $u(t)$ is again the Heaviside unit-step function. To evaluate S_2, we first substitute (20) in (24) to yield

$$S_2(r;t) \simeq -\frac{i}{2\pi}\int_0^{\infty}\frac{dv}{R_o}\int_{\infty}^{\infty}\frac{e^{it_{ro}[\omega(\omega+i2\lambda_o)]^{\frac{1}{2}}}}{[\omega(\omega+i2\lambda_o)]^{\frac{1}{2}}}e^{-i\omega t_{vo}}\,d\omega$$

where $t_{ro} = R_o/c_o$; R_o is defined in (19), $t_{vo} = t - v/c_o$ and λ_o is written in (18). The integrand of the second integral has two branch points for $\omega = 0$ and $\omega = -i2\lambda_o$. The choice of the branch cut will be along the negative imaginary axis as shown in Fig. 2 in order that $[\omega(\omega+i2\lambda_o)]^{\frac{1}{2}} \to \omega$ as $|\omega| \to \infty$. Deformation of the above contour into the upper half of the complex ω-plane for $(t_{vo} - t_{ro}) < 0$ will give zero, since the integrand is analytic in the upper half-plane. Only for $(t_{vo} - t_{ro}) \geq 0$, we can deform the real axis integration into the lower

half-plane. This means that

$$\frac{r}{c} \leq t \leq [v_o + R_o(v_o)]/c_o \tag{29}$$

where

$$v_o = [-\frac{\tau}{n} + \sqrt{(1 + \frac{1}{n^2})\,\tau^2 - r^2}]/n$$

and $\tau = c_o t$. Evaluation of the integral around the branch cut yields the form of

$$S_2(r;t) = -\frac{1}{2\pi}\int_o^{v_o}\frac{dv}{R_o}\int_o^{-2i\lambda_o} e^{-i\omega t_{vo}}\cos t_{ro}\,|\omega(\omega+i2\lambda_o)|^{\frac{1}{2}} \cdot \frac{d\omega}{|\omega(\omega+i2\lambda_o)|^{\frac{1}{2}}}$$

It should be noted that the first integral was truncated up to v_o because of the causality criterion (i.e. for $t < (v+R_o)/c_o$ the second integral goes to zero). Now using $\omega = -i\lambda_o(1-\cos\theta)$ and after some mathematical manipulation, the above integral reduces simply to [18]

$$S_2(r;t) = -\int_o^{v_o}\frac{dv}{R_o}\, e^{-\lambda_o t_{vo}}\, I_o(\lambda_o\sqrt{t_{vo}^2 - t_{ro}^2})\; u(t-r/c_o) \tag{30}$$

where I_o is the Modified Bessel function of zero order.

The advantage of the above form for $S_2(r;t)$ is that now we have a single finite integral instead of a double infinite integral and it can be easily evaluated numerically. We note that with the exception of setting $N(\omega) = 1$ the above integral expression is exact. Evaluation of $S_4(r;t)$ follows basically the same procedure as applied to $S_2(r;t)$. However, because of the presence of additional branch cut with branch points at $\omega = 0$ and $\omega = -2i\Delta$ care must be exercised in taking the value of the square

roots along the deformed path. As derived in the Appendix, the result is given as follows:

$$S_4(r;t) = \frac{1}{n}\int_o^{v_1} \frac{dv}{R_1}\, e^{-\lambda_1 t}\, I_o(\lambda_1\sqrt{t^2-(v+R_1)^2/c_1^2})\cdot u(t-\frac{r}{c_1}) \qquad (31)$$

where

$$v_1 = n\,[-\tau + \sqrt{(1+1/n^2)^2 - r^2}]; \quad \tau = c_o t \qquad (32)$$

R_1 and λ_1 are defined in (22) and c_1 is the speed of light in the earth medium (i.e. $c_1 = c_o/n$). Again, it should be noted that we have succeeded in transforming the double infinite integrals of $S_4(r;t)$ into a single finite limit one through the deformation of the path in the complex λ-plane. These reulsts can be easily calculated using straightforward numerical techniques.

4. Analytical Expression for a Lossless Half-Space

For a lossless earth, the conductivity $\sigma = 0$ and therefore the inverse of the relaxation time $\Delta = 0$ also. Hence, the expression $S_j(r;t)$, $j = 1,2,3,4$ as given in (2.39), (2.43), (2.44) and (2.45) respectively, reduces to the following form

$$S_1(r;t) = \frac{1}{t_o}\,(t-t_o)\,u(t-t_o)$$

$$S_2(r;t) = -\int_o^{v_o} \frac{dv}{R_o}\, u(t-t_o)$$

$$S_3(r;t) = -\frac{1}{n\,t_1}\,(t-t_1)\,u(t-t_1)$$

$$S_4(r;t) = \frac{1}{n}\int_o^{v_1} \frac{dv}{R_1}\, u(t-t_1)$$

Using the above relations for $S_j(r;t)$ and the relation in (25) for the vector potention with an impulse current source, we can write $\pi_z(r;t)$

as follows:

$$\pi_z(r;t) = 60\, nc_o I_o d\ell \left[\frac{n}{r} u(t-t_o) - \frac{1}{nr} u(t-t_1) \right.$$

$$\left. \frac{u(t-t_o)\, u(t_1-t)}{\sqrt{(1+1/n^2)^2 - r^2}} \right]$$

The above time response for $\pi_z(r;t)$ is exactly that of the well known solution obtained by Van der Pol [6] for a vertical dipole on the surface of a non-conducting half-space.

5. Numerical Results

A computer program was set up to find the real time solution of the electric vector potential as derived in (26) for an impulse function current source. The program utilizes the solutions obtained for $S_j(r;t)$, $j = 1,2,3$, and 4 as given by the expressions in (27), (28), (30), and (31) respectively. The z-component of the electric field and the ϕ-component of the magnetic field are obtained from the expressions given in (2) and (3). Due to the complex form of the vector potential $\pi_z(r;t)$ numerical differentiations are used. By choosing suitable increments of r and t results accurate to the order of the increments square can be attained.

In Figures 5 and 6, we have plotted the individual terms that contribute to the pulse shape of the electric and magnetic field respectively as a function of observation times $(t - t_o)$ for an observation distance $r = 100$ m and conductivity $\sigma = 10^{-3}$ mho/m. The dielectric constant of earth ε_r is assumed to be 10 and $t_o = r/c_o$ is the arrival time of the first pulse. e_j and h_j; $j = 1,2,3,4$ correspond to the four terms that contribute to the electric and magnetic field as $S_j(r;t)$, $j = 1,2,3,4$

correspond to the four terms of the vector potential $\pi_z(r;t)$. It is clear that the dominant term for the intermediate and later times is $-e_1$ (shown as dashled lines). However, at the early time portion of the pulse, say $t - t_o < 0.2$ μsec, e_2 is the dominant field. The major cause of distortion and dispersion is associated with this term. The other contributions e_3 and e_4 have an arrival time $t \geq t_1 = nr/c_o$ corresponding to transmission through the earth medium. These terms usually are of the same order of magnitude and their difference in general is smaller than e_2. Even for cases where their difference is larger than e_2, the total sum $(e_2 + e_3 - e_4)$ is a lot less than e_1. For larger distances, e_3 and e_4 can be shown to be even smaller.

The ϕ-component of the magnetic field as shown in Fig. 6 however shows that the second term h_2 is the dominant contributor to the field since $h_1 \equiv 0$ as in the case for the electric field. The later time arrival solutions h_3 and h_4 usually have a difference smaller than h_2. Their contributions can be shown to be even smaller for larger distances.

From these results, we came to the conclusion that for a typical earth parameter and for observation distances greater than 100 m, the arrival of the pulse from the earth are negligible for all practical purposes. A two term approximation in the electric $(-e_1 + e_2)$ and a one term solution in the magnetic field $(-h_2)$ should suffice a reasonable answer to the field above a lossy half-space.

Figures 7 through 8 show the total electric field $E_z(r;t)$ as a function of time $(t-t_o)$ for two conductivities ($\sigma = 10^{-2}$, 10^{-3} mho/m) and for three observation distances r = 0.1 and 1 km respectively. In the first graph (i.e. Fig. 7), a linear scale for the electric field is plotted as a function of a logarithmic scale in time. As expected, the

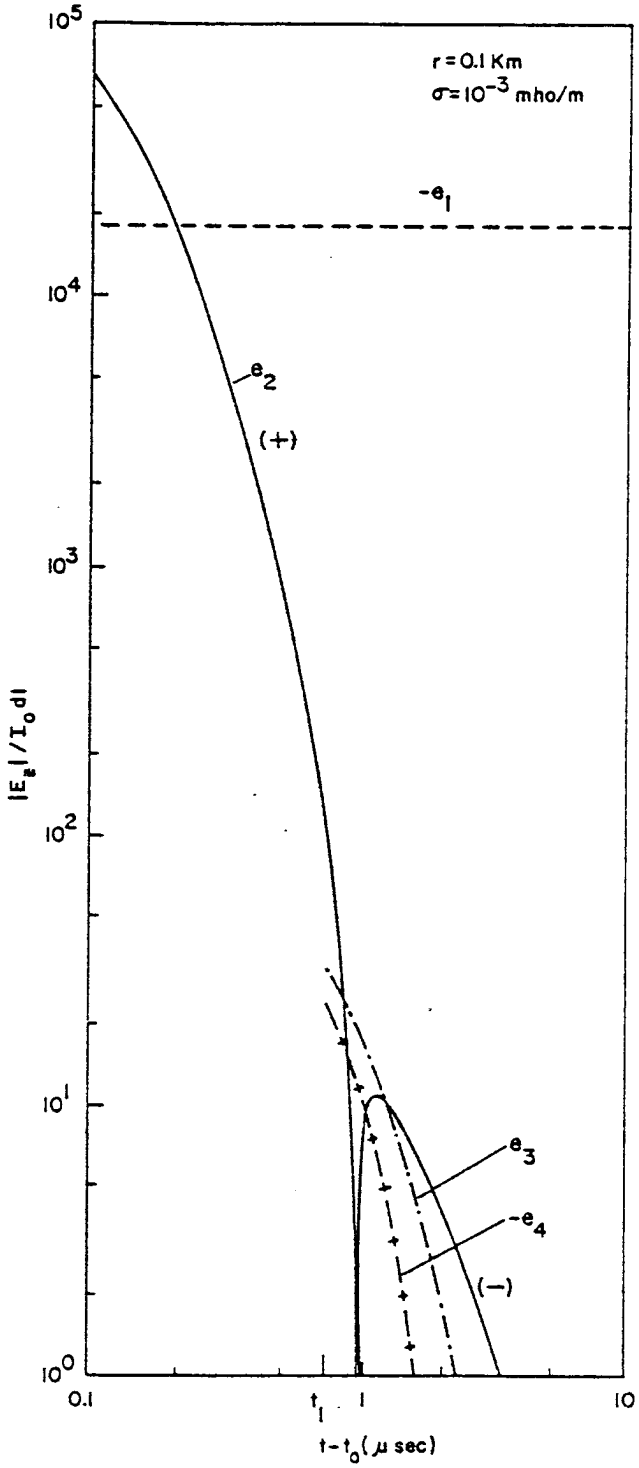

Figure 5. Comparison of the individual arrival terms for the electric field at a distance r = 100 m. The (+) and (-) signs refer to positive and negative polarity, respectively. $t_1 = nr/c_o$, is the time of arrival of the pulse from the earth medium.

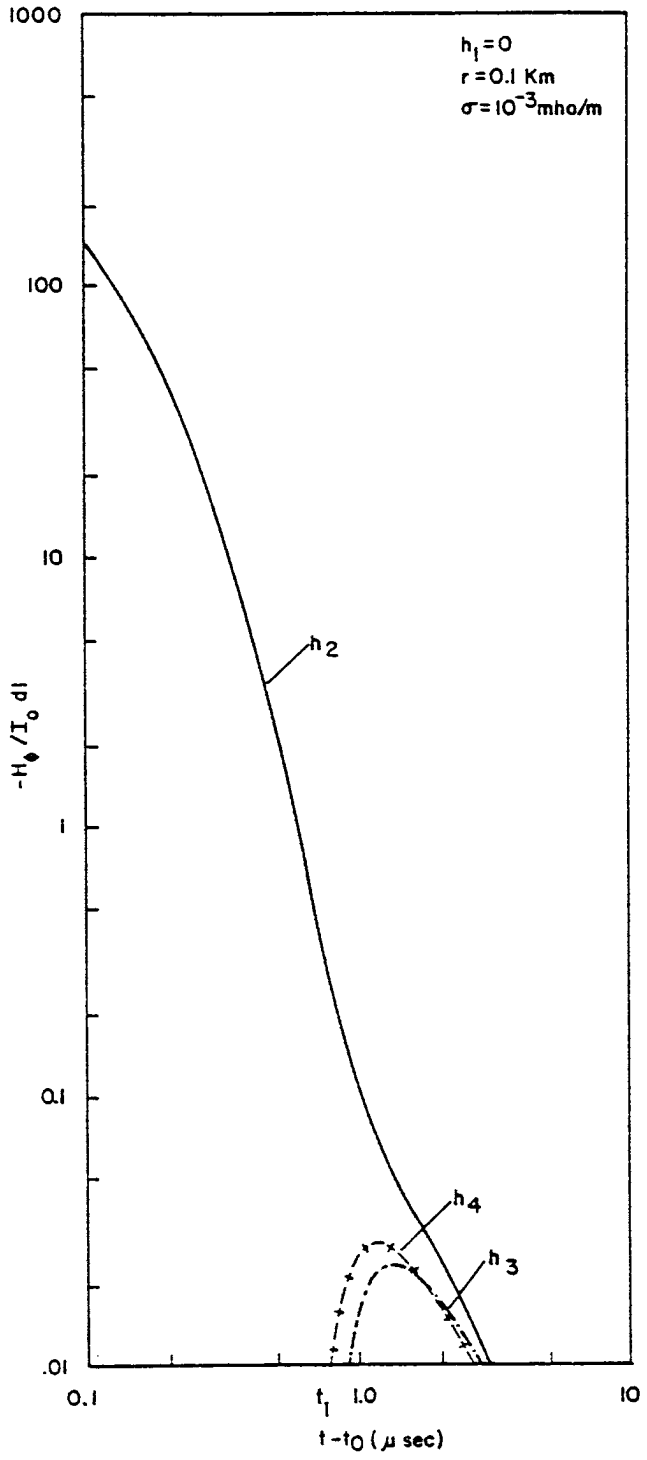

Figure 6. Comparison of the individual arrival terms for the ϕ-component of the magnetic field at a distance r = 100 m; $t_1 = nr/c_o$ is the time of arrival of the pulse from the earth medium.

two curves, representing two different conducting media, reach the constant level of the static field shortly after the time t_1. A similar though a logarithmic scale in the electric field is shown in Figure 11 for observation distance of 1 km. The influence of the earth on the dispersion of the propagating pulse is more clearly observed at this distance. For $\sigma = 10^{-3}$ mho/m, the peak has shifted from $t - t_o = 0.2$ μsec. Also, the early segment of the pulse is broader and attenuated due to the loss in the medium. Again, the pulse levels off to a negative constant for later observation times.

In Figs. 9 to 10 we have here, similar to the electric field plots, the ϕ-component of the magnetic fields. The behavior of the pulse is almost the same as that of the electric field except it decays continuously to zero for a later observation time. Figure 11 compares the electric field with an approximate formula derived from [10] as a function of observation time $(t - t_o)$ for a distance $r = 10$ km and for two different conductivities $\sigma = 10^{-2}$ and 10^{-3} mho/m. These results agree very well for times $t - t_o \leq 0.1$ μsec. Also, they agree fairly well in their overall pattern behavior for all times. However, there are disagreements in the magnitude of the peaks and the observation times of the peaks and nulls. This is not surprising, since the approximation in [10] is basically that of an early-time one. Note that the response approaches to that of a perfectly-conducting ground at the later times. To examine more closely the effect of the ground conductivity, we have plotted in Figs. 12 and 13 the electric field E_z versus the inverse of conductivity (i.e. σ^{-1}) for 4 different observation times $t - t_o$ (1,2,4 and 8 μ sec) and for $r = 0.1$, 10 km respectively. The first graph shows that for short observation distance, earth, which typically has a conductivity between 10^{-3} t- 10^{-2} v/m, acts

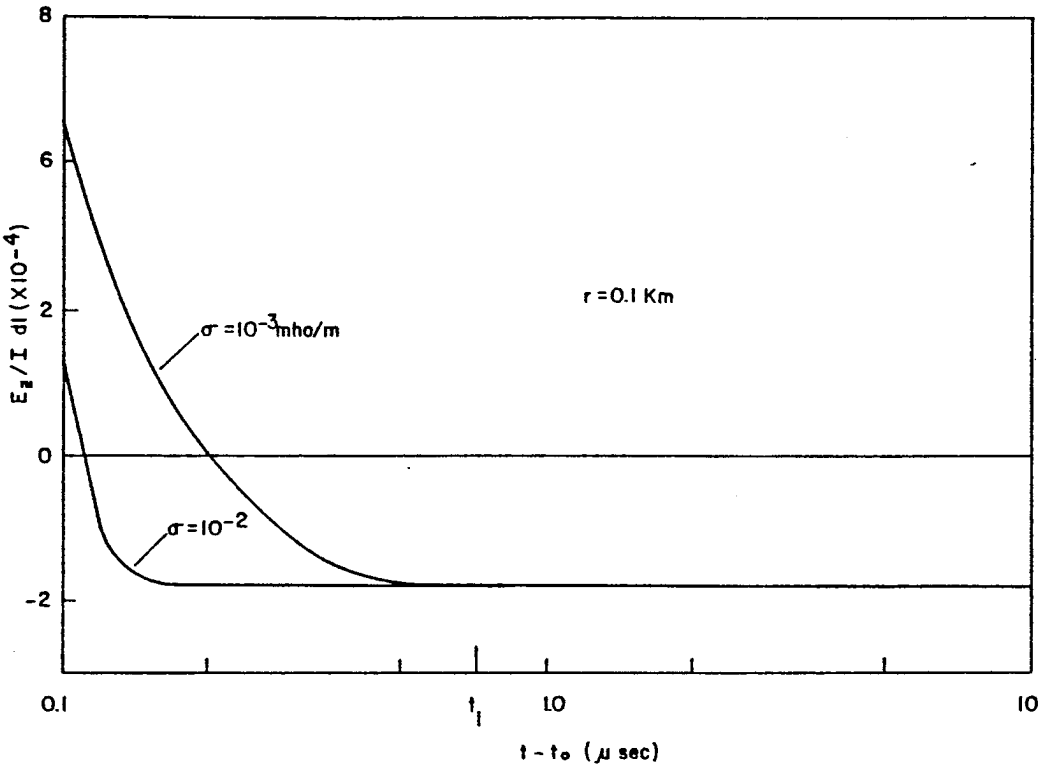

Figure 7. Vertical electric field versus observation time $(t-t_o)$ at r = 100 m for two different conductivities; $t_1 = nr/c_o$ is the time of arrival of the pulse from the earth medium.

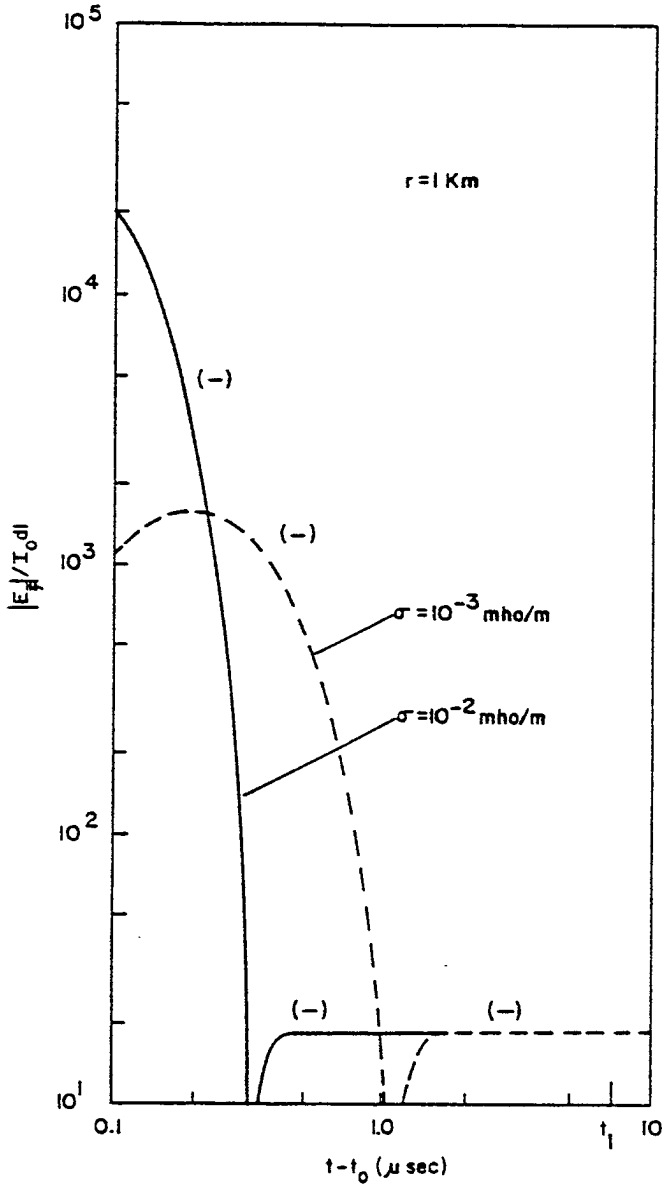

Figure 8. Vertical electric field versus observation time $(t-t_o)$ at r = 1 km for two different conductivities. The (+) and (−) signs refer to positive and negative polarity, rexpectively. $t_1 = nr/c_o$ is the time of arrival of the pulse from the earth medium.

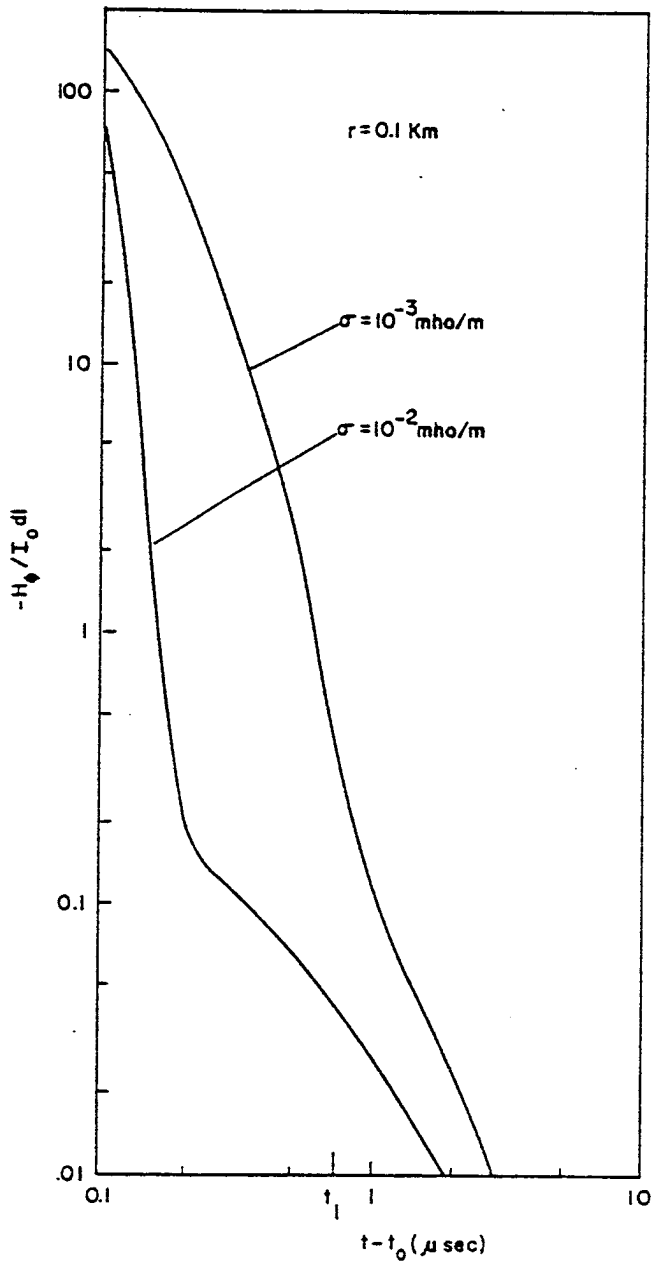

Figure 9. Transverse magnetic field versus $(t-t_o)$ at $r = 100$ m for two different conductivites; $t_1 = nr/c_o$ is the time of arrival of the pulse from the earth medium.

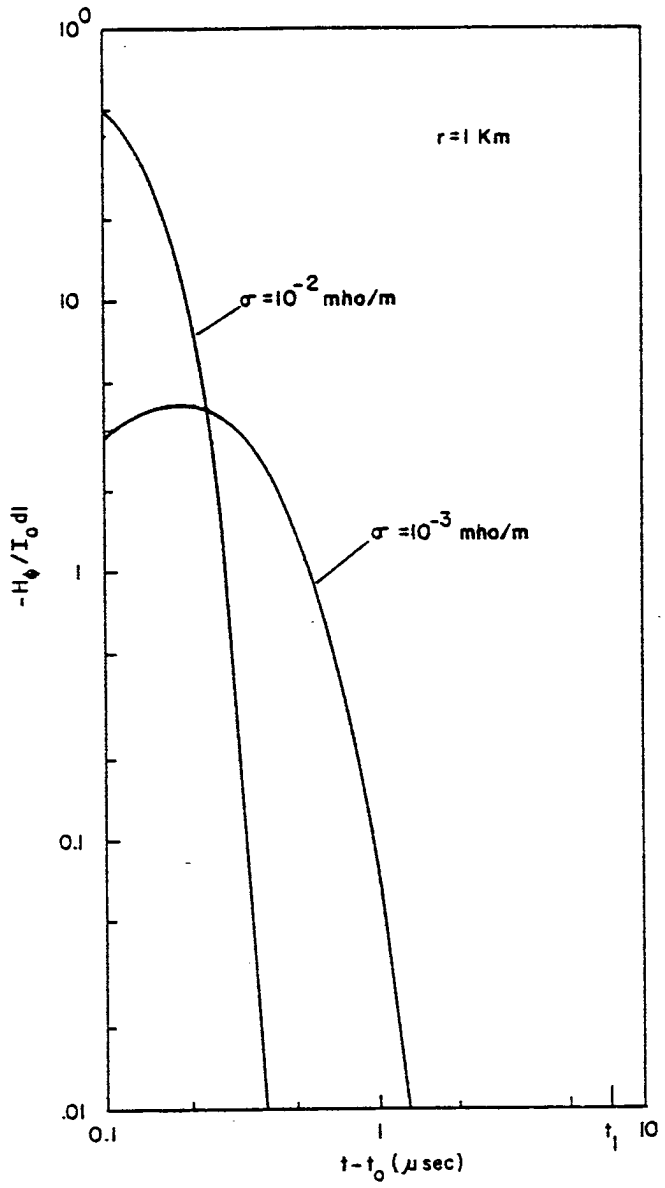

Figure 10. Transverse magnetic field versus $(t-t_o)$ at r = 1 km for two different conductivities; $t_1 = nr/c_o$ is the time of arrival of the pulse from the earth medium.

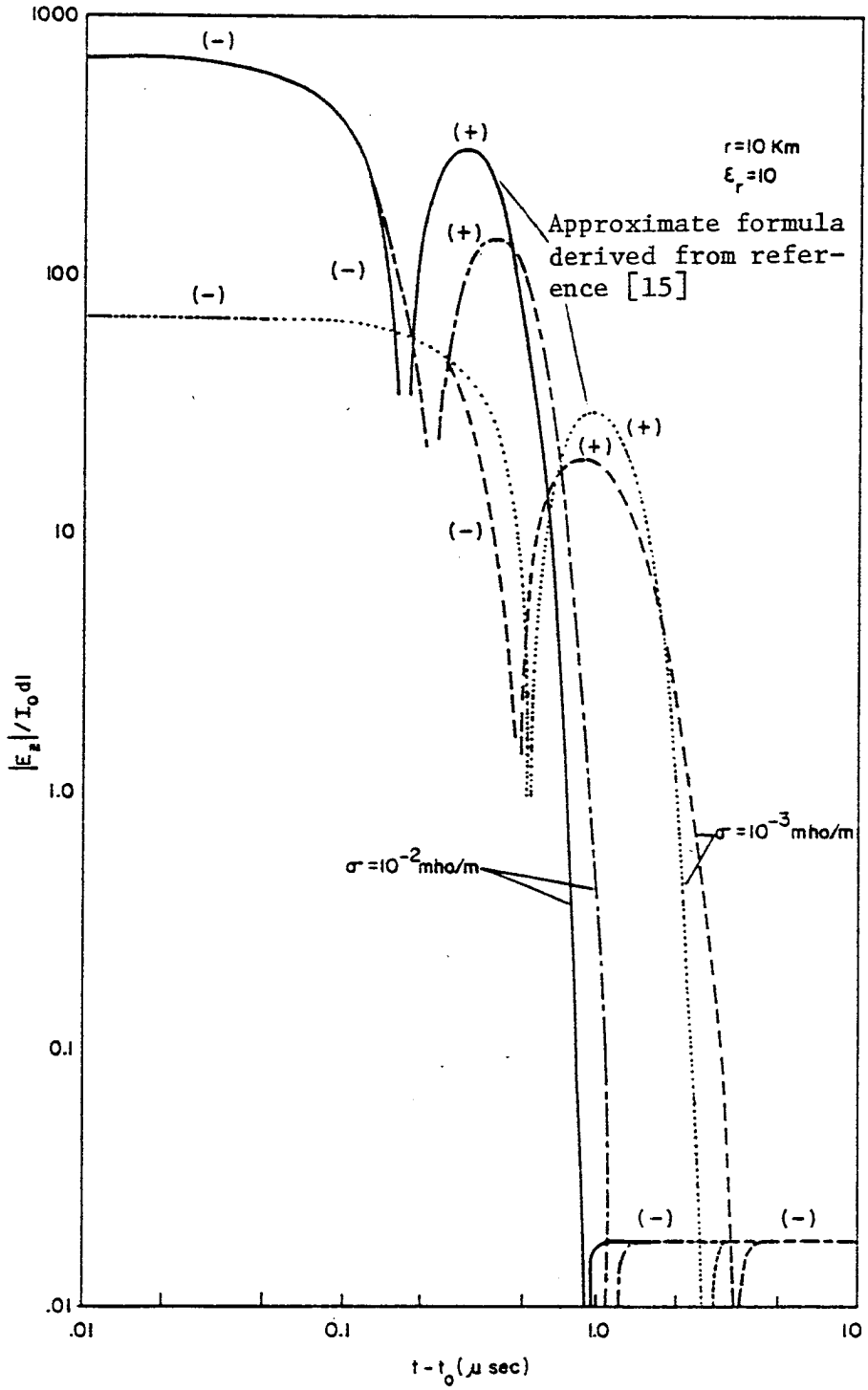

Figure 11. Comparison between the early time solution based on reference [15] and the solution obtained by substituting (2.39) and (2.43)-(2.45) into (2.37b) and then using the Maxwell relation in (2.15). The (+) and (-) signs refer to positive and negative polarity, respectively.

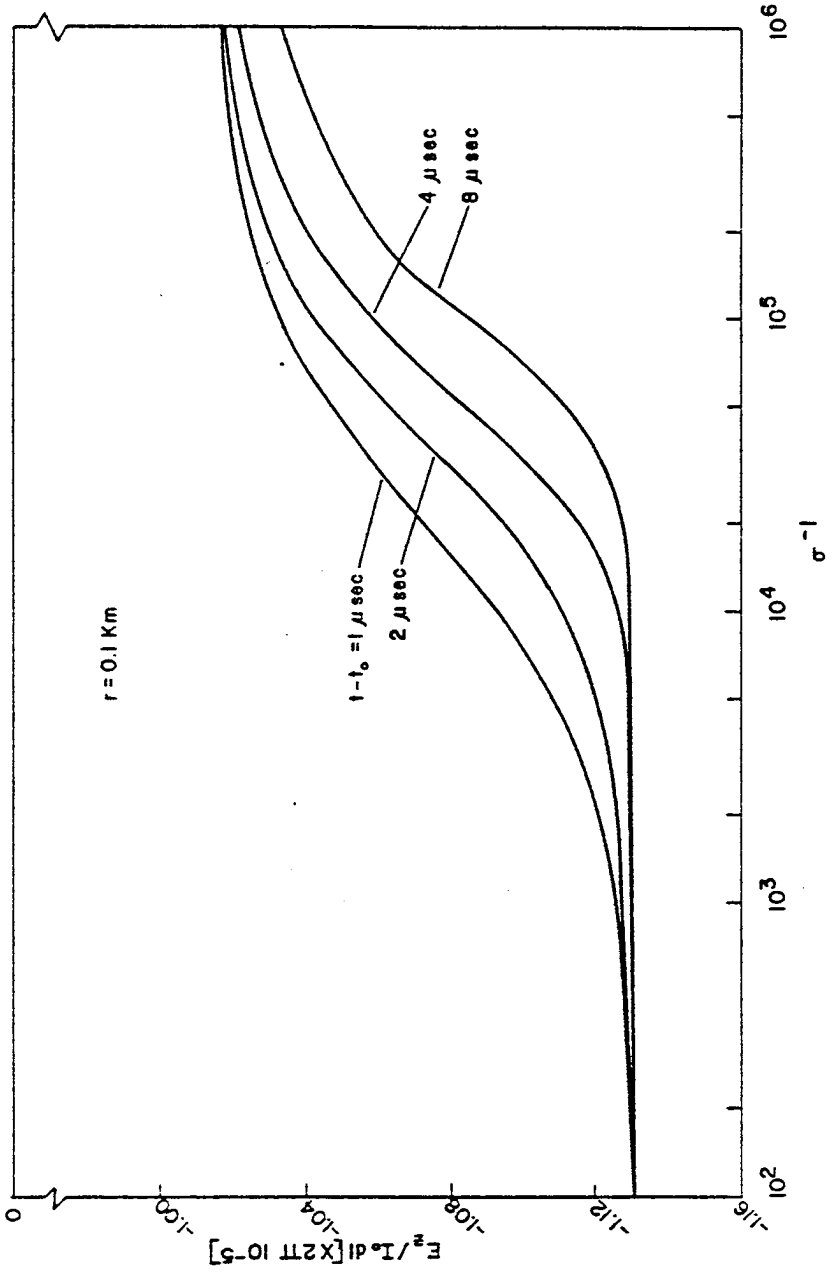

Figure 12. Vertical electric field versus ground conductivity for 4-different observation times ($t-t_o$) at r = 100 m.

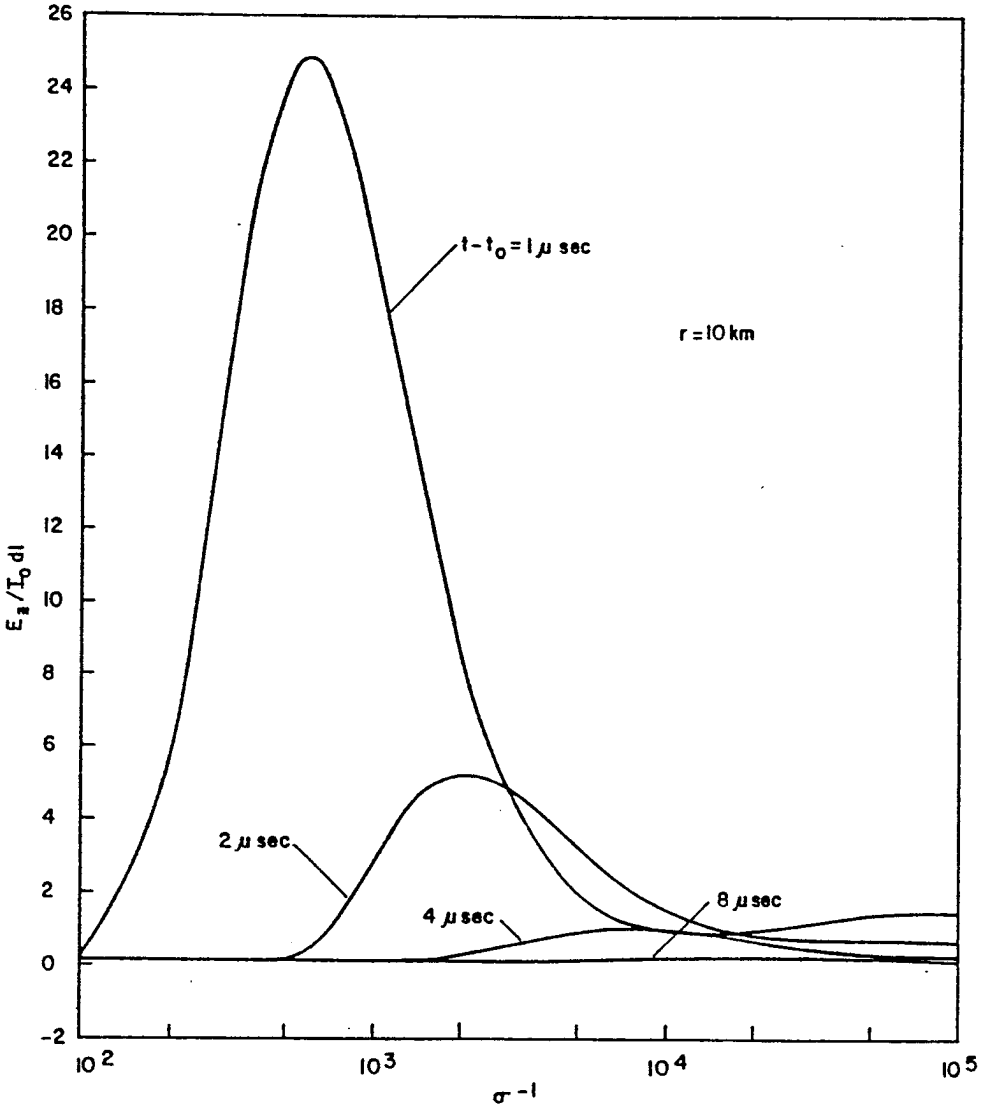

Figure 13. Vertical electric field versus ground conductivity for 4-different observation times ($t-t_o$) at r = 10 km.

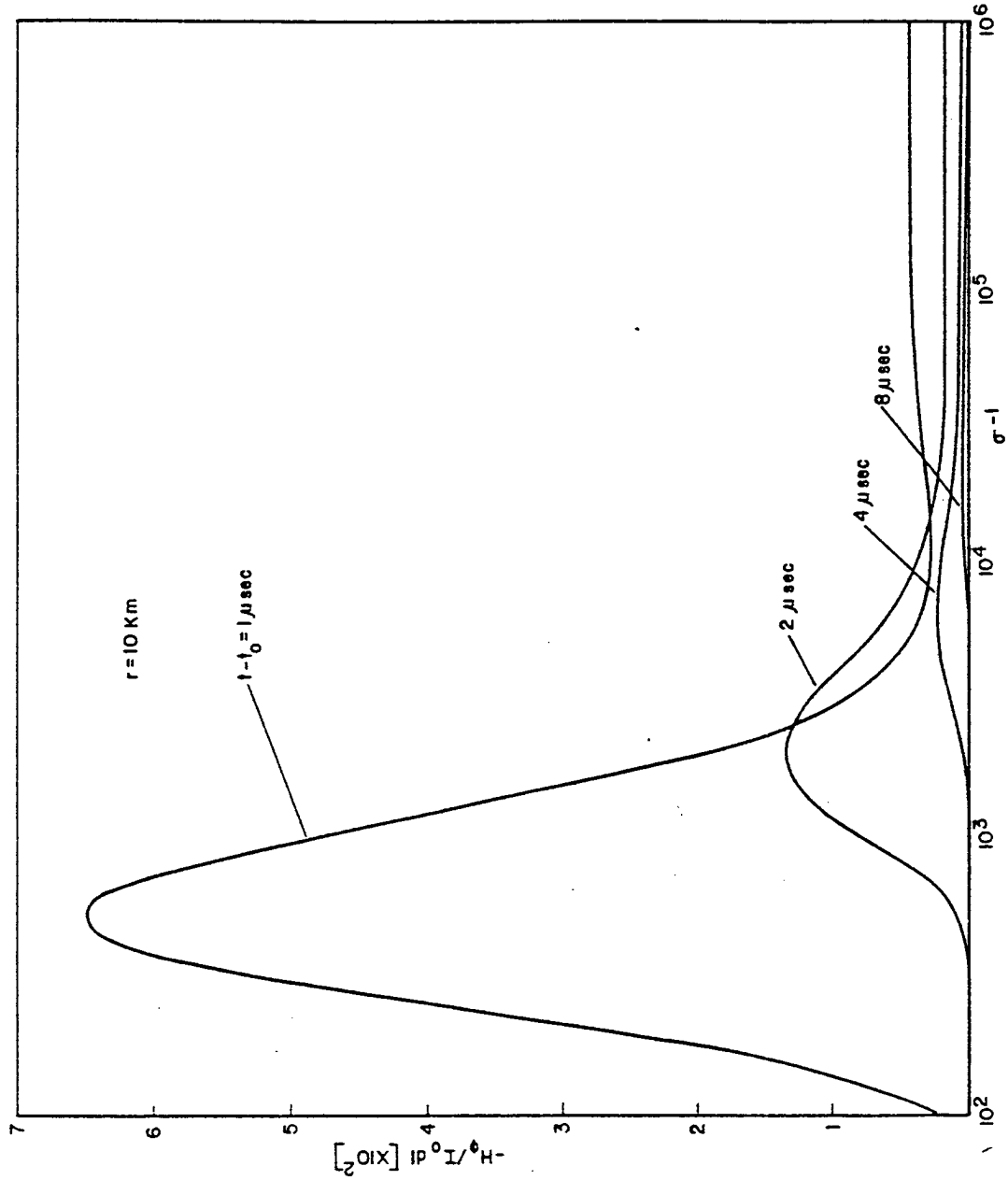

Figure 15. Transverse magnetic field versus ground conductivity for 4-different observation times ($t-t_o$) at r = 10 km.

REFERENCES

[1] Special Joint Issue on the Nuclear Electromagnetic Pulse (EMP), IEEE Tran. Antennas Propagat., vol. AP-26, no. 1, Jan. 1978.

[2] J.R. Wait (ed.), Electromagnetic Probing in Geophysics, Boulder, Colo., The Golem Press, 1971.

[3] M. A. Uman and D.K. McLain, "Lightning return stroke current from magnetic and radiation field measurements," J. Geophysical Res., vol. 75, pp. 5143-5147, Sept. 1970.

[4] J. R. Johler, "Propagation of pulse from nuclear burst," IEEE Trans. Antennas Propagat., vol. AP-15, no. 2, pp. 256-264, March 1967.

[5] D. L. Moffatt and R. K. Mains, "Detection and discrimination of radar targets," IEEE Trans. Antennas Propagat., vol. AP-23, pp. 358-367, May 1975.

[6] B. Van der Pol, "On discontinuous electromagnetic waves and the occurrence of surface wave," IRE Trans. Antennas Propagat., vol. 4, pp. 288-293, 1956.

[7] B. Van der Pol and A.H.M Levelt, "On the propagation of a discontinuous electromagnetic wave," Ned. Akad. Wetensch. Proc. Ser. A 63 = Indag. Math., vol. 22, pp. 254-265, 1960.

[8] H. Bremmer, "The pulse solution connected with the Sommerfeld problem for a dipole in the interface between two dielectrics," Electromagnetic Waves, R. E. Langer ed., pp. 39-64, The U. of Wisconsin Press, 1962.

[9] J. R. Wait, "Transient fields of a vertical dipole over a homogenous curved ground," Can. J. Phys., vol. 34, pp. 27-35, 1956.

[10] J. R. Wait, "Propagation of electromagnetic pulses in terrestrial wave guides," IEEE Trans. Antennas Propagat., vol. AP-13, no. 6, pp. 904-918, 1965.

[11] V.V. Novikov, "Propagation of pulsed signals over a homogenous flat earth," Radio Eng. Elect. Phys., vol. 8, pp. 299-301, 1963.

[12] D. C. Chang, "Electromagnetic pulse propagation over a conducting earth," Technical Report no. 8, Electromagnetics Lab., Dept. of Elec. Eng., U. of Colo., Boulder, C) 80309, April 1973.

[13] J. R. Wait, "On the electromagnetic pulse response of a dipole over a plane surface," Can. J. Phys., vol. 52, pp. 193-196, 1974.

[14] J. A. Fuller and J. R. Wait, "A pulsed dipole in the earth," Transient Electromagnetic Fields, L. B. Felsen ed., New York, Springer-Verlag, 1975.

[15] A. Baños, Dipole Radiation in the Presence of a Conducting Half-Space, Pergamon, Oxford, 1966.

[16] A. Sommerfeld, Partial Differential Equations in Physics. vol. VI, p. 246, Academic Press, 1949.

[17] M. Abramowitz and I. A. Stegun, Handbook of Mathematical Functions, pp. 377 and 297, Dover, New York, 1964.

[18] I. S. Gradshteyn and I. M. Ryzhik, Table of Integrals Series Products, 4th Ed., Academic Press, New York, 1965.

Acknowledgment

We would like to thank Prof. J.R. Wait for his comments and suggestions. The work is mainly based upon the first author's Ph.D. Thesis. Partial support from the Air Force Weapons Laboratory, Albuquerque, N.M. under a subcontract OT-0122 with the Institute of Telecommunication Sciences is also acknowledged.

APPENDIX A

THE SOLUTION TO THE DOUBLE INTEGRAL EXPRESSION OF $S_4(r;t)$

Upon the substitution of (21) into (24) and the subsequent use of the approximation $N(\omega) \simeq 1$, we can write the integral expressions for $S_4(r;t)$ as

$$S_4(r;t) = \frac{1}{n} \left(\frac{i}{2\pi}\right) \int_o^\infty \frac{dv}{R_1} \int_{-\infty}^{\infty} \frac{e^{it_{r2}[\omega(\omega+i2\lambda_1)]^{\frac{1}{2}}}}{[\omega(\omega+i2\lambda_1)]^{\frac{1}{2}}} \cdot e^{it_{vl}[\omega(\omega+i2\Delta)]^{\frac{1}{2}}} e^{-i\omega t} \, d\omega \qquad \text{A.1}$$

where $t_1 = r/c_1$, $t_{r1} = R_1/c_1$, $t_{vl} = v/c_1$ and R_1 and λ_1 are defined in (22). Here, $c_1 = c_o/n$ is the speed of light in the earth medium.

The integrand over ω contains two branch cut singularities; one is associated with the square root function; $[\omega(\omega+i2\lambda_1)]^{\frac{1}{2}}$, and the other with the function $[\omega(\omega+i2\Delta)]^{\frac{1}{2}}$. The two branch cuts are shown in Fig. 2. A similar procedure to the evaluation of $S_2(r;t)$ as presented in section (3) is followed here. The integrand is holomorphic in the upper half of the complex ω-plane and thus for $t < (R_1+v)/c_1$, the integral contribution is zero. For $t \geq (R_1+v)/c_1$, we may deform the integration countour into the lower half-plane thereby obtaining two branch cut integrals. We note that $\arg[\omega(\omega+i2\lambda_1)]^{\frac{1}{2}}$ and $\arg[\omega(\omega+i2\Delta)]^{\frac{1}{2}}$ are both o on one side of the cut and π on the other side for ω between o and $-2i\lambda_1$. However,